INSTYTUT FIZYKI JĄDROWEJ
INSTITUTE OF NUCLEAR PHYSICS
ИНСТИТУТ ЯДЕРНОЙ ФИЗИКИ

KRAKÓW

RAPORT No 1242/PH

EVIDENCE FOR A NON-$q\bar{q}$ TENSOR MESON AT 1410 MeV PRODUCED IN THE REACTION $\pi^- p \to K_S^0 K_S^0 n$ AT 63 GeV

C. Daum, L. Hertzberger, W. Hoogland, S. Peters,
P. Van Deurzen, A. Berglund, V. Chabaud,
A. Gonzalez–Arroyo, B. Hyams, H. Tiecke, P. Weilhammer,
A. Dwurażny, H. Pałka, G. Polok, K. Rybicki, M. Turała,
J. Turnau, A. Zalewska, H. Becker, G. Blanar, M. Cerrada,
H. Dietl, J. Gallivan, M. Gelubman, R. Klanner, E. Lorenz,
G. Lütjens, G. Lutz, W. Männer, A. Pugl, U. Stierlin,
J. Blakey, M. Bowler, R. Cashmore, J. Loken, J. Spalding,
G. Thompson, B. Alper, C. Damerell, A. Gillman, J. Hardwick,
F. Wickens

KRAKÓW 1984

EVIDENCE FOR A NON-$q\bar{q}$ TENSOR MESON AT 1410 MeV PRODUCED IN THE REACTION $\pi^- p \rightarrow K^0_s K^0_s n$ AT 63 GeV

ACCMOR COLLABORATION

C. Daum, L. Hertzberger, W. Hoogland, S. Peters, P. Van Deurzen
NIKHEF-H, 1009 DB Amsterdam, The Netherlands

A. Berglund, V. Chabaud, A. Gonzalez-Arroyo, B. Hyams,
H. Tiecke, P. Weilhammer
CERN, 1211 Geneva 23, Switzerland

A. Dwurazny, H. Palka, G. Polok, K. Rybicki, M. Turala,
J. Turnau, A. Zalewska
Institute of Nuclear Physics, 30-055 Krakow, Poland

H. Becker, G. Blanar, M. Cerrada, H. Dietl, J. Gallivan,
M. Gaidbman, R. Klanner, E. Lorenz, G. Lütjens, G. Lutz,
W. Männer, A. Pugl, U. Stierlin
Max-Planck-Institut für Physik und Astrophysik, Werner Heisenberg Institut für Physik, D-8 München-40, Federal Republic of Germany

J. Blakey, M. Bowler, R. Cashmore, J. Loken, J. Spalding,
G. Thompson
Oxford University, Nuclear Phys. Lab., Oxford OX1 3NP, UK

B. Alper, C. Damerell, A. Gillman, J. Hardwick, F. Wickens
Rutherford Appleton Lab., Chilton, Didcot, Oxon OX11OQX, UK

Abstract

We present an analysis of the $K_S^0K_S^0$ system produced in the reaction $\pi^- p \to K_S^0K_S^0 n$ at 63 GeV based on $\sim$700 events in the kinematical region of $|t| < 0.5\ GeV^2$. We concentrate on masses between 1200 and 1600 MeV where a double maximum structure is observed. Performing an amplitude analysis in this mass interval we find that S, D_0 and D_+ waves contribute to the mass spectrum at approximately equal strength. The peaks are attributed to spin 2 waves. However, we failed to explain them by interfering f(1270), A_2(1310) and f'(1520) resonances alone. While the first peak can be associated with f(1270) - A_2(1310) production, an additional tensor meson is needed with mass of $\sim$1410 MeV and a narrow width for a description of the second one. The analysis as well as the energy dependence deduced from some published $K_S^0K_S^0$ mass spectra suggests this object to be dominantly produced by a natural parity exchange. Because the $2^{++}q\bar{q}$ nonet is already complete the nature of the new tensor meson is an open question.

1. Introduction

With glueball search gaining momentum and first candidates claimed in J/ψ radiative decays /1,2/ a need for a complete understanding of the hadron spectrum in the low energy region populated by light quark resonances becomes more evident. This is the main reason for which we have decided to publish some data which cannot be explained by any simple quark model. Namely we present the data for the reaction $\pi^- p \to K^0_S K^0_S n$ at 63 GeV, showing a peculiar behaviour in the f(1270) - A_2(1310) - f'(1520) region of the $K^0_S K^0_S$ effective mass. The data suggest an additional state around 1410 MeV. Although statistics in this experiment seems to be insufficient to unambiguously claim a new state, we corroborate our observations with many other experiments in which the effect was apparently in the data but has never been paid much attention except for reference /3/ where a new 2^{++} state at 1440 MeV has been postulated.

The discovery of the 2^{++} Θ(1690) meson in radiative J/ψ decays: $J/\psi \to \gamma \eta\eta$ and $J/\psi \to \gamma K\bar{K}$ makes it a natural candidate for the gluonium related state, however, its interpretation is still an open question /4/. Clearly, other candidates for a ground state spin 2 gluonium have to be also considered. We do not know if the effect we observe has anything in common with gluonium but we stress again that good understanding of the spectroscopic data in the region of glueball-quarkonium mixing is absolutely necessary before one can claim "beyond any reasonable doubt" the finding of a new type of hadron matter - gluonium state.

The paper is organized as follows: In Section 2 we describe the experiment. The data for the reaction $\pi^- p \to K^0_S K^0_S n$ at 63 GeV and the analysis are presented in Section 3. Section 4 contains a discussion of $K\bar{K}$ data from other experiments at different energies. The paper is closed with conclusions.

2. The experiment and data reduction

The reaction

$$\pi^- p \to K^0_s(\to\pi^+\pi^-) K^0_s(\to\pi^+\pi^-) n \quad (1)$$

has been measured with the ACCMOR spectrometer at the CERN SPS as part of an extensive experimental program devoted to high statistics studies of peripheral collisions. The data were recorded simultaneously with the reactions:

$$\pi^- p \to \pi^+\pi^- n \quad (2)$$

$$\pi^- p \to K^+K^- n \quad (3)$$

$$\pi^- p \to p\bar{p} n \quad (4)$$

$$K^- p \to K^+K^- \Lambda(\Sigma) \quad (5)$$

The apparatus was a double magnet large aperture spectrometer based on wire spark chambers and proportional chambers. The layout of the spectrometer is shown in Fig. 1. A detailed description of the spectrometer was published elsewhere /5/. Here we describe only those aspects of the experimental procedure which were essential for the measurement of reaction (1).

The experiment was performed using a 63 GeV unseparated negative beam incident on a 50 cm liquid hydrogen target. The beam was defined by a set of scintillation counters and its π^-, K^- and $\bar{p}$ content tagged with two differential and one threshold counters. The target was surrounded by a system of lead-scintillator sandwich counters (F) which served to select events with a recoil neutron. Information from these counters was not included into the trigger for reaction (1) but was used in the off-line analysis. A 0.2 cm thick scintillation counter D_1 placed at the end of the target selected events with neutrals produced in forward direction. A decay volume for K_s^o was defined by requiring at least 2 signals in the scintillation hodoscope P2/3. The momenta of the pions from the K_s^o decays were measured in the spectrometer formed by two magnets of bending power of 0.8 Tm and 2 Tm respectively and five sets of wire spark chambers with magnetostrictive read-out. The production of additional mesons in a forward direction and at large angles was detected by lead-scintillator sandwich counters G and F.

The trigger for reaction (1) was designed to select interactions producing initially neutral final states where at least one particle decayed subsequently into charged particles. These requirements were fulfilled by demanding an incoming particle interacting in the target and no signal from the D_1 counter coinciding with at least two signals in the P2/3 counter array and the absence of any signal in the lead-scintillator sandwich counters G.

We recorded a total of 269 000 "neutral" triggers. The sensitivity of the experiment was 25 events/nb.

The data were processed off-line with our track reconstruction and V_o-search programs. Events with a double-vee topology were tested for kinematical consistency of each V_o with a K_s^o, Λ or $\overline{\Lambda}$ decay. Neutral vees were accepted as K_s^o decays if the effective mass for the $\pi^+\pi^-$ hypothesis was between 0.481 and 0.518 GeV while the effective mass for the

$p\pi^-$ ($\bar{p}\pi^+$) hypothesis was outside of the Λ ($\bar{\Lambda}$) mass region: $1.110 < m_\Lambda < 1.122$ GeV. Events with a recoiling neutron were selected first by demanding no signal in the outer layer of F-counters and further by requiring that the square of the missing mass (MM^2) was in the interval $-1.1 < MM^2 < 2.1$ GeV^2.

The $K_s^0 \to \pi^+\pi^-$ mass spectrum and the MM^2 distribution for events with two accepted K_s^0 decays are shown in Figs 2 and 3. From these distributions we estimate that after applying the cuts the sample contains a negligible contamination of Λ's (4%) and events with an additional π^0 (3%). Our invariant mass resolution is below 20 MeV for $K_s^0K_s^0$ masses below 1600 MeV. The MM^2 resolution is ~ 0.4 GeV^2.

The sample has been corrected for acceptance losses by the following Monte Carlo method. For each detected event we generated randomly decay distances of both K_s^0 and their decay azimuthal angles. Further the event was rotated by a random angle around its beam particle direction. The beam energy spread and primary vertex distribution were also taken into account in the calculations. We could use this method of acceptance calculation because our spectrometer had no acceptance holes for events with both K_s^0's decaying inside the decay volume. The calculated acceptance is decreasing for increasing invariant $K_s^0K_s^0$ mass. For masses $1200 < m_{K\bar{K}} < 1600$ MeV it is typically around 40%. The events were further corrected for losses due to δ-ray production (8%) and neutrons detected by the F-counters (7%).

The final data sample consists of ~ 700 events for reaction (1).

3. Results

In Fig. 4 we show the observed and corrected $K_s^oK_s^o$ mass spectrum for $-t < 0.5$ GeV^2 in 30 MeV bins. The structure in the effective $K_s^oK_s^o$ mass spectrum can be divided into three distinct regions: the threshold region ($m_{K\bar{K}} < 1200$ MeV), a pronounced structure between 1200 and 1600 MeV with two prominent peaks at 1300 and 1400 MeV and a much less populated high mass region.

This paper deals with the region between 1200 and 1600 MeV. The broad structure in this region has been observed in all previous $K_s^oK_s^o$ and K^+K^- experiments at lower energies (see Section 4), however the double-maximum pattern present in our data is a new feature.

In Fig. 5 we show the unnormalized spherical harmonic moments of the decay angular distributions calculated in the Gottfried-Jackson frame in 60 MeV mass bins. Since for masses below 1600 MeV the acceptance is nonvanishing over the full angular range we computed the moments simply by evaluating $N \langle Y_L^m \rangle = \sum w_i Y^m(\theta_i, \varphi_i)$ where w_i is the weight of the i-th event. This weight includes the inverse of the acceptance and topology-dependent corrections.

We present the moments up to $L = 4$ and $M \leq 2$ since those with higher L and $M > 2$ were all found to be consistent with zero in the considered mass region. The moments can be expressed as linear combinations of bilinear products of the helicity amplitudes with a definite exchanged parity - $L_{\pm m}$

$$N \langle Y_0^0 \rangle = S^2 + D_0^2 + D_+^2 + D_-^2 \qquad (6a)$$

$$N \langle Y_2^0 \rangle = 2SD_0 + 0.639 D_0^2 + 0.319(D_+^2 + D_-^2) \qquad (6b)$$

$$N\langle Y_2^1\rangle = 1.414\, SD_- + 0.452\, D_0 D_- \qquad (6c)$$

$$N\langle Y_2^2\rangle = 0.391\,(D_-^2 - D_+^2) \qquad (6d)$$

$$N\langle Y_4^0\rangle = 0.857\, D_0^2 - 0.571\,(D_-^2 + D_+^2) \qquad (6e)$$

$$N\langle Y_4^1\rangle = 1.107\, D_0 D_- \qquad (6f)$$

$$N\langle Y_4^2\rangle = 0.452\,(D_-^2 - D_+^2) \qquad (6g)$$

where for amplitudes L we use a spectroscopic nomenclature (S, D) and adopt a shorthand notation for the unnatural parity exchange (UPE) amplitudes $L_0 = L_{-0}$, $L_- = L_{-1}$ and $L_+ = L_{+1}$ for the natural parity exchange (NPE) amplitudes. Terms L^2 and L_1L_2 stand for $|L|^2$ and $\mathrm{Re}\,(L_1L_2^*)$ respectively. Each amplitude consists of two independent amplitudes: a nucleon helicity flip ($L_{\pm m;+-}$) and a nonflip ($L_{\pm m;++}$) amplitude. Since we do not measure the polarization of the nucleon, summation over target helicity is implied such that $L^2 = |L_{\pm m;+-}|^2 + |L_{\pm m;++}|^2$ and $L_{\pm m}L'_{\pm m'} = \mathrm{Re}(L_{\pm m;++}L'^{*}_{\pm m';++} + L_{\pm m;+-}L'^{*}_{\pm m';+-})$.

Because of the modest statistics of our sample the moments have large errors even at 60 MeV binning. Therefore a reliable analysis of moments which would reveal a detailed mass dependence of amplitudes was not possible. Nevertheless we attempted to solve the set of equations (6) mainly with the aim to estimate the contributions of the individual amplitudes to the total cross-section. Combining equations (6d) and (6g) the set (6) is reduced to a system of six equations for six unknown quantities (S^2, D_0^2, D_+^2, D_-^2, $\cos\varphi_{SD_0}$, $\cos\varphi_{SD_-}$) which can be solved analytically in each mass bin. The system has two physical solutions: a "phase coherent" solution for which

$\cos\varphi_{SD_-} \approx -1.0$ and an "incoherent" one ($\cos\varphi_{SD_-} \approx 0.0$). If the commonly accepted "phase coherent" solution is chosen one obtains the following cross-sections of individual waves integrated over the mass interval 1200 - 1560 MeV: $\sigma_S = 57 \pm 17$ nb, $\sigma_{D_0} = 77 \pm 12$ nb, $\sigma_{D_+} = 45 \pm 10$ nb, $\sigma_{D_-} = 4 \pm 6$ nb. The quoted numbers include a correction for unseen K^0_s decays as well as for the $K^0_L K^0_L$ mode. The errors are statistical only while the systematic error of the cross-section is below 10%.

Although the errors are large it is clear that for our data the D_+ amplitude is nearly as important as S and D_0 amplitudes while the amount of D_- is negligible.

We refrain from interpretation of the mass dependence of the extracted amplitudes because of huge statistical errors. Instead, we attempt a mass dependent fit to mass spectrum and moments using a simple ansatz for J = 0 and J = 2 waves. Its formulation is based on the results of the energy independent analysis.

To simplify the problem we do not consider all of the amplitudes involved. Firstly, we neglect the D_- wave which was found to be consistent with zero. Secondly, we do not attempt to determine the content of the S-wave which is still controversial (/6/ and /7/ under entry ε(1300)). Instead, we assume that the intensity of this wave is best given by an interpolation of all existing high statistics results. In Fig.6 we show a compilation from Ref. /8/ of the S-wave intensities from $K^0_s K^0_s$ analyses of Refs /8/, /9/ and /10/. The only reasonable conclusion which can be drawn from this plot is that the $|S|^2$ forms a broad maximum centered at around 1300 MeV and this cannot influence the narrow effects in the mass spectrum. For purpose of our ansatz we approximate this wave with a simple formula which reproduces the $|S|^2$ shape as found in

$K_s^0K_s^0$ analyses (see the curve in Fig. 6). Thus only D_0 and D_+ amplitudes are determined.

The amplitudes were parametrized by Breit-Wigner expressions:

$$BW_R = C_R \frac{m_R \Gamma^R_{K\bar{K}}}{m^2_{K\bar{K}} - m^2_R - i m_R \Gamma^R_{TOT}} \qquad (7)$$

where: C_R is a normalization constant

m_R - mass of the resonance

$\Gamma^R_{K\bar{K}}$, Γ^R_{TOT} - its partial and total widths

$m_{K\bar{K}}$ - invariant $K_s^0K_s^0$ mass.

Because of the proximity of resonance masses and thus importance of interferences between the resonances, we have tried various parametrizations for widths: starting from the simplest case where $\Gamma_{K\bar{K}}$ and Γ_{TOT} are proportional to full formulas where the numerator of the Breit-Wigner amplitude contains partial widths for initial and final state interaction ($\sqrt{\Gamma_{in}\Gamma_{out}}$) and Γ_{TOT} is approximated by main decay channel. In some fits the formulas for widths had phase space behaviour only ($\Gamma \propto q^5$, with $q = (m^2_{K\bar{K}}/4 - m^2_K)^{1/2}$, in others they contained also J = 2 Blatt-Weisskopf function.

In the first step we attempted to describe the mass spectrum in terms of known states f(1270), A_2(1310) and f'(1520). We assume that f(1270) and f'(1520) are described by UPE amplitudes (π-exchange) and A_2(1310) is produced dominantly by NPE i.e.

$$D_0 = BW_f + BW_{f'} e^{i\varphi_{ff'}}$$

$$D_+ = BW_{A_2} \qquad (8)$$

The positions and widths of f(1270) and A_2(1310) resonances have been fixed at their PDG values /7/. For the mass and width of f'(1520) meson we used the values determined from measurements of reactions $K^-p \to K^+K^-\Lambda(\Sigma)$ and $K^-p \to K^0_sK^0_s\Lambda$, because only these reactions allow straightforward observations of f'(1520) (see discussion in Ref. /14/). We have chosen the following f'(1520) parameters: $m_{f'}$ = 1523 MeV, $\Gamma_{f'}$ = 73 MeV. The phase $\varphi_{ff'}$ between f and f' amplitudes has been fixed at 180°. This corresponds to the assumption that f'(1520) is produced by the same mechanism as f(1270). In some of our fits the phase was allowed to vary but it always stayed around 180°. The result of the fit is shown in Fig. 5. The fit yielded an unacceptable χ^2 of 37/12 d.f. The main contribution to the χ^2 ($\sim$23) comes from the structure in the mass spectrum around 1410 MeV. The deviation from the fitted curve corresponds to an effect of 9 st. dev. In some fits $N\langle Y_4^0\rangle$, $N\langle Y_4^1\rangle$ and $N\langle Y_4^2\rangle$ moments were included as well. They have large errors, therefore they were correctly reproduced by every fit (see a broken line for moments in Fig. 5). However, an overall χ^2 was still bad ($\sim$53/36 d.f.) again acquiring its main contribution from the mass spectrum at 1410 MeV.

Failing to describe the mass spectrum with known mesons we introduced a new 2^{++} state which we will call further G(1410). We did not fix a production mechanism of G allowing both UPE and NPE components. Thus the fitted amplitudes were the following:

$$D_0 = BW_f + BW_{f'}e^{i\varphi_{ff'}} + k\,BW_G e^{i\varphi_{fG}}$$

$$D_+ = BW_{A_2} + BW_G e^{i\varphi_{A_2G}} \qquad (9)$$

where k stands for UPE/NPE ratio for G(1410).

The results of the fit for different parametrizations of the widths are shown in Table I. Parameters which were fixed are quoted without errors. One representative result of the fits (fit A) is displayed in Fig. 5 as a continuous line. As it can be seen from Table I and Fig. 5 the fits describe very well the mass spectrum and the main features of the moments. Different parametrizations of the widths are of minor importance for the results of the fit. From fit B we conclude that G(1410) is dominantly produced by NPE with less than 10% of UPE component. In Fig. 7 we show the interference term between $A_2(1310)$ and G(1410). It has a specific shape which enhances the double peak structure.

The amount and helicity composition of the f(1270), $A_2(1310)$ and f'(1520) production resulting from the fit can be compared with the expectations from studies of the other reactions.

The f(1270) production at 63 GeV can be estimated from our $\pi^+\pi^-$ data of reaction (2) taken with the same spectrometer simultaneously with reaction (1). This channel offers a nearly pure f(1270) signal, because the f'(1520) is strongly suppressed (OZI rule) and $A_2(1310)$ is forbidden in the decay channel (G-parity). The analysis of the $\pi\pi$ data yielded a D_0-wave cross-section integrated over the mass interval 1200 - 1600 MeV equal to $\sigma_{\pi\pi}(D_0) = 1.78 \pm 0.04$ μb. Applying the branching ratio BR($f \rightarrow K\bar{K}/f \rightarrow \pi\pi$) $\approx$ 3.5% /7/ we get for the neutral K^0K^0 mode: $\sigma(f \rightarrow K^0\bar{K}^0) = 40.9 \pm 2.9$ nb as compared to $\sigma(f \rightarrow K^0\bar{K}^0) = 56.5 \pm 11.3$ nb predicted by the fit. The intensities of the D_- and D_+ waves for $\pi\pi$ data are small and do not exceed 5% and 15% of the $|D_0|^2$ respectively.

The amount of the $A_2(1310)$ production at our energy can be estimated from measurements of the reactions $\pi^+ n \rightarrow \pi^+\pi^-\pi^0 p$ and $\pi^- p \rightarrow \pi^-\pi^+\pi^0 n$ at 12 and 15 GeV /11/. The measurement at 15 GeV yielded $\sigma(\pi^- p \rightarrow A_2 n \rightarrow \pi^-\pi^+\pi^0 n) = 7.9 \pm 1.0\ \mu b$ for $-t < 0.5\ \mathrm{GeV}^2$, $1200 < m_{3\pi} < 1500$ MeV and an UPE/NPE ratio of ~ 0.7. Scaling the UPE component with p_{LAB}^{-2} and the NPE component with p_{LAB}^{-1} to 63 GeV momentum and using $BR(A_2 \rightarrow K\bar{K}) \approx 5\%$ /11/ we expect in our data ~ 5 nb of $A_2(1310)$ production by UPE and ~ 26 nb of $A_2(1310)$ production by NPE. The last number again agrees very well with the $\sigma(A_2 \rightarrow K^0\bar{K}^0) = 30.6 \pm 6.2$ nb resulting from the fit.

The exact amount of the $f'(1520)$ cannot be estimated. From the compilation of $K\bar{K}$ analyses (Table V of Ref. /8/) one can deduce $\sigma(f')/\sigma(f) = 0.25^{+0.09}_{-0.04}$ (all the analyses assumed OPE mechanism for the $f'(1520)$ production). This number, however, depends significantly on the $f'(1520)$ position and width which differ for various analyses. Our fit predicts $\sigma(f' \rightarrow K^0\bar{K}^0) = 18 \pm 7$ nb which is equivalent to $\sigma(f')/\sigma(f) \sim 0.3$. The NPE component of the $f'(1520)$ production is unknown. However, it is presumably small because the NPE production of known mesons decreases substantially with increasing meson mass.

To summarize: the presented above estimates agree with the results of the fit and represent a consistency check for our analysis.

4. Comparison with other $K^0_S K^0_S$ results

In Fig. 8 we present a compilation of published $K^0_S K^0_S$ mass spectra at different beam momenta. Only experiments with reasonable statistics have been included to the compilation. The data of Beusch et al. /11/ at 6.2 GeV are not corrected for acceptance.

All the mass spectra have a pronounced shoulder or a second peak on the high mass side of the dominant peak, which becomes more and more evident as the energy increases. The energy dependence of the mass spectra would suggest that NPE production mechanism is responsible for splitting the bump at the highest energies. The NPE production mechanism would also explain why the majority of the analyses of the lower energy data did not require a new tensor meson to describe this mass region.

Only in one of early studies at 5, 7 and 12 GeV /3/ the enhancement around 1400 MeV has been interpreted as a fourth state (besides f(1270), A_2(1310) and f'(1520)). These data have never been fully analysed in terms of moments, but a simple Breit-Wigner fit to the mass spectrum yielded the mass of the state at $\sim$1440 MeV and width 40 $\pm$ 20 MeV.

Amongst all of the data presented in Fig. 8 only for those at 6 and 7 GeV /9/, 8.9 GeV /10/ and 23 GeV /8/ amplitudes analyses have been performed.

Polychronakos et al. /9/ have performed an energy independent amplitude analysis of their 6 and 7 GeV data for $-t < 0.2$ GeV^2. They have assumed that the amplitudes are nucleon-spin coherent and that D_- and D_0 are phase coherent. Having extracted intensities of individual waves they were able to describe the D_0 amplitude by f(1270) + f'(1520) contributions only with the f'(1520) position fixed to 1515 MeV. We note however that, as can be seen in Fig. 17 of Ref. /9/, the D_+ amplitude is quite substantial for masses 1350 - 1450 MeV being at least at a level of 25% of the D_o-wave intensity in the same mass interval.

The data of Ref. /10/ have been analysed in terms of reggeised parametrization based on OPE model with absorption. The extracted D_o wave was found to be satisfactorily described by the f(1270) meson alone. However, as was pointed out by authors themselves /10/ the model has apparent difficulties in describing $N\langle Y_4^1\rangle$ and $N\langle Y_4^2\rangle$ moments. In our opinion the same concerns the $N\langle Y_4^0\rangle$ moment for masses above 1400 MeV.

The recent data of Etkin et al. /8/ at 23 GeV which represents the highest statistics for reaction (1) have been analysed also in the framework of OPE for $-t < 0.1\ GeV^2$. The authors conclude that the resulting D_+ and D_- amplitudes are small and negligible. Subsequently, performing mass dependent fits to moments they succeeded in describing the D_o amplitude by f(1270), A_2(1310) and f'(1520) contributions with f' parameters fixed to $m_{f'}$ = 1525 MeV and $\Gamma_{f'}$ = 90 MeV. However, even with the large f' width they were unable to describe a significant peak which (Fig. 4 of Ref. /8/) appears at ~1450 MeV in their $N\langle Y_4^0\rangle$ moment.

The effect, although less spectacular, seems to be present also in the reaction $\pi^- p \to K^+K^-n$. As it was pointed out in Ref. /15/, a description of $N\langle Y_4^0\rangle$ moment of CERN-Munich data at 17.2 GeV and 18.4 GeV, as well as the Argonne data at 6 GeV /16/, needed an f' position below 1500 MeV and a large width. If the f' parameters were fixed to the PDG table values (from 1980 edition: $m_{f'}$ = 1515 MeV, $\Gamma_{f'}$ = 65 MeV) a fourth D_o-wave object had to be introduced with the following parameters: $m = 1422 \pm 9$ MeV and $\Gamma = 80 \pm 42$ MeV. The same data have been recently reanalysed in Ref. /14/ incorporating information of polarization and using $m_{f'} = 1523$ MeV, $\Gamma_{f'} = 73$ MeV. The fits yielded $m = 1436^{+26}_{-16}$, $\Gamma = 81^{+56}_{-29}$ and A_1-exchange as a possible production mechanism.

Our K^+K^- data at 63 GeV /17/ essentially have the same features as those at 18.4 GeV but indicate a presence of larger NPE component. Again the mass spectrum cannot be described by a broad S-wave and a superposition of the f(1270), A_2(1310) and f'(1520) states alone. The ansatz of the equation (9) yielded similar results as that for $K^0_sK^0_s$ channel, except for the larger G(1410) width ($m = 1422 \pm 11$, $\Gamma = 177 \pm 47$) /17/. The larger width is a consequence of the fact that in the K^+K^- mass spectrum the effect does not appear as a pronounced narrow peak like in $K^0_sK^0_s$ data. If G(1410) is an isospin singlet state the reason for that might be the specific interference pattern between A_2(1310) and G(1410) ($I = 1$ and $I = 0$ amplitude respectively) as found in our $K^0_sK^0_s$ fit. For K^+K^- data the interference term is expected to change sign and thus the splitting between f(1270) - A_2(1310) and G(1410) peaks disappears (see Fig. 7 for the predicted interference term). Thus the fit to both channels together, independently of providing stronger constraints, allows additionally determination of the isospin of the new state. However, the analysis of K^+K^- data is much more complex because of contributions from P- and F-waves. Such simultaneous analysis of both data sets assuming that the P-wave is negligible has been performed in Ref. /17/. The analysis yielded a $I = 0$ G(1410) meson with parameters $m = 1412 \pm 3$ MeV and $\Gamma = 14 \pm 6$ MeV.

5. Summary and conclusions

We have tried to interpret the $K_s^0 K_s^0$ mass spectrum for reaction (1) at 63 GeV in the mass region of the f(1270), A_2(1310) and f'(1520). Contrary to the analyses at lower energies /8-10/ we are not able to describe the data by these three mesons and a broad S-wave alone. The reason is the pronounced peak which appears in our mass spectrum at $\sim$ 1410 MeV where in the low energy data only a small enhancement or a shoulder was present. The position of the peak is far below the f'(1520) mass, thus its interpretation as a result of interference of a rather narrow f'(1520) with the f(1270) or A_2(1310) mesons is rather improbable. Interpreting the peak as a new tensor meson we have obtained a good description of the mass spectrum and moments. The parameters of this new object are a mass of 1410 MeV and a width of 10-35 MeV. The analysis and the fact that the peak becomes stronger with increasing energy suggest the NPE production mechanism for this state. Such a production mechanism would explain why G(1410) has not been required in high statistics $K_s^0 K_s^0$ data at lower energies.

An additional spin 2 state has been claimed also for K^+K^- data /15,14,17/. Its parameters agree within errors with ours. Isospin of G(1410) depends on production mechanism. The analyses /15,12,17/ came to different conclusions on the production mechanism (π-, A_1-exchange and NPE) of G(1410). The analysis of Ref. /17/, pointing to the NPE production mechanism, was able to determine the isospin of the state as I=0. The I=0 assignment for this state is supported also by the fact that no structure around 1400 MeV has been seen in $\pi^- p \rightarrow K^- K_s^0 p$ data /18/.

In order to confirm the existence of G(1410) and to establish its quantum numbers new investigations are clearly needed. The best choice would be a high statistics experiments studying simultaneously reactions

$$\pi^- p \to K^+ K^- n$$
$$\pi^+ n \to K^+ K^- p$$
$$\pi^- p \to K^0_s K^0_s n$$
$$\pi^+ n \to K^0_s K^0_s p$$

which allows full separation of isospin amplitudes.

REFERENCES

/1/ D. Sharre et al., Phys. Lett. 97B, 329 (1980).

/2/ E.D. Bloom, in Proc. of XXI Int. Conf. on High Energy Physics, ed. by P. Petiau, M. Porneuf, Paris 1982, pp. 407-430.

/3/ W. Beusch et al., Phys. Lett. 25B, 357 (1967).

/4/ H.J. Schnitzer, Nucl. Phys. B207, 131 (1982).

/5/ C. Daum et al., Nucl. Phys. B182, 269 (1981).

/6/ A. Etkin et al., Phys. Rev. D25, 2446 (1982).

/7/ Particle Data Group, Phys. Lett. 111B (1982).

/8/ A. Etkin et al., Phys. Rev. D25, 1786 (1982).

/9/ V.A. Polychronakos et al., Phys. Rev. D19, 1317 (1979).

/10/ W. Wetzel et al., Nucl. Phys. B115, 208 (1976).

/11/ M.J. Corden et al., Nucl. Phys. B138, 235 (1978).

/12/ W. Beusch et al., in Experimental Meson Spectroscopy, ed. by C. Baltay and A.H. Rosenfeld, Columbia University Press 1970, pp. 185-195.

/13/ G.N. Baloshin et al., Yad. Fiz. 24, 567 (1976).

/14/ V. Chabaud et al., Nucl. Phys. B223, 1 (1983).

/15/ V. Chabaud et al., Acta Phys. Pol. B12, 575 (1981).

/16/ A.J. Pawlicki et al., Phys. Rev. D15, 3196 (1977).

/17/ H. Palka, Ph.D. Thesis, Institute of Nuclear Physics, Cracow 1983, Raport No 1230/PH.

/18/ A.D. Martin et al., Nucl. Phys. B140, 158 (1978); A.D. Martin et al., Phys. Lett. 74B, 417 (1978).

TABLE I

Results of the tensor mesons interference fits

Resonance	Parameters	Fit A*	Fit B**
f(1270)	C_f [(nb/30 MeV)$^{1/2}$]	$2.96^{+1.58}_{-1.68}$	$2.75^{+0.24}_{-0.34}$
	m_f [MeV]	1273	1273
	Γ_f [MeV]	179	179
A_2(1310)	C_{A_2} [(nb/30 MeV)$^{1/2}$]	$2.31^{+0.30}_{-0.34}$	$2.45^{+0.28}_{-0.32}$
	m_{A_2} [MeV]	1318	1318
	Γ_{A_2} [MeV]	110	110
f'(1520)	$C_{f'}$ [(nb/30 MeV)$^{1/2}$]	$1.90^{+0.39}_{-0.41}$	$2.49^{+0.49}_{-0.57}$
	$m_{f'}$ [MeV]	1523	1523
	$\Gamma_{f'}$ [MeV]	73	73
	$\cos\varphi_{f'f}$	-1.0	-1.0
G(1410)	C_G [(nb/30 MeV)$^{1/2}$]	5.92 ± 2.57	$4.7^{+5.21}_{-2.51}$
	m_G [MeV]	1407^{+5}_{-4}	1411^{+6}_{-4}
	Γ_G [MeV]	13^{+14}_{-3}	15^{+20}_{-10}
	$\cos\varphi_{GA_2}$	1.00 ± 0.01	1.00 ± 0.02
	$\cos\varphi_{Gf}$	-	0.58 ± 0.20
	k	0.0	0.06 ± 0.06
	χ^2/n.d.f.	31.4/32	32.4/30

*In this fit Γ^R_{TOT} was approximated by the width for a main decay channel of the resonance ($\pi\pi$ for f(1270), $\rho\pi$ for A_2(1310), $K\bar{K}$ for f'(1520) and G(1410)). For the partial width we used formulas for $K\bar{K}$ channel. In both cases: $\Gamma \sim (q/q_o)^5 \cdot D_2(q^oR)/D_2(qR)$ with R = 5 GeV^{-2}.

**Here Γ^R_{PART} was assumed to be proportional to Γ^R_{TOT}. Phase space dependence and centrifugal barrier effects have been taken into account as previously (with $K\bar{K}$ kinematics).

Figure captions

Fig. 1. Layout of the spectrometer: H_2 - hydrogen target; MNP, BBC - spectrometer magnets; I, II, IIIa, IIIb, IIIc - wire spark chamber sets; F, G, H - lead-scintillator sandwich counters; D_1 - scintillation veto counter; P1, P2/3 - hodoscopes for multiplicity selection; Č1, Č2 - gas Čerenkov counters

Fig. 2. The $\pi^+\pi^-$ effective mass distribution. The arrows indicate the mass range of events selected as K_s^0

Fig. 3. The missing mass-squared spectrum of $K_s^0K_s^0$ events. The arrow indicates the cut for neutron-recoil selection

Fig. 4. The $K_s^0K_s^0$ effective mass spectrum for $-t < 0.5$ GeV^2. The histogram refers to raw data. Points with error bars show corrected events

Fig. 5. The acceptance corrected, unnormalized t-channel moments $N \langle Y_L^M \rangle$ as functions of invariant mass for $-t < 0.5$ GeV^2. --- The fit to the mass spectrum with f(1270), A_2(1310) and f'(1520) mesons only. — The best fit with the G(1410) included

Fig. 6. Comparison of the intensities of S-wave as found in $K_s^0K_s^0$ analyses of Refs /9/, /10/ and /11/ taken from Ref. /9/. The solid line denotes a simple B-W parametrization which was used in fits described in the text

Fig. 7. The interference term G(1410) A_2(1310) for $K_s^0K_s^0$ and prediction for K^+K^-

Fig. 8. Compilation of published $K_s^0K_s^0$ mass spectra at different beam momenta

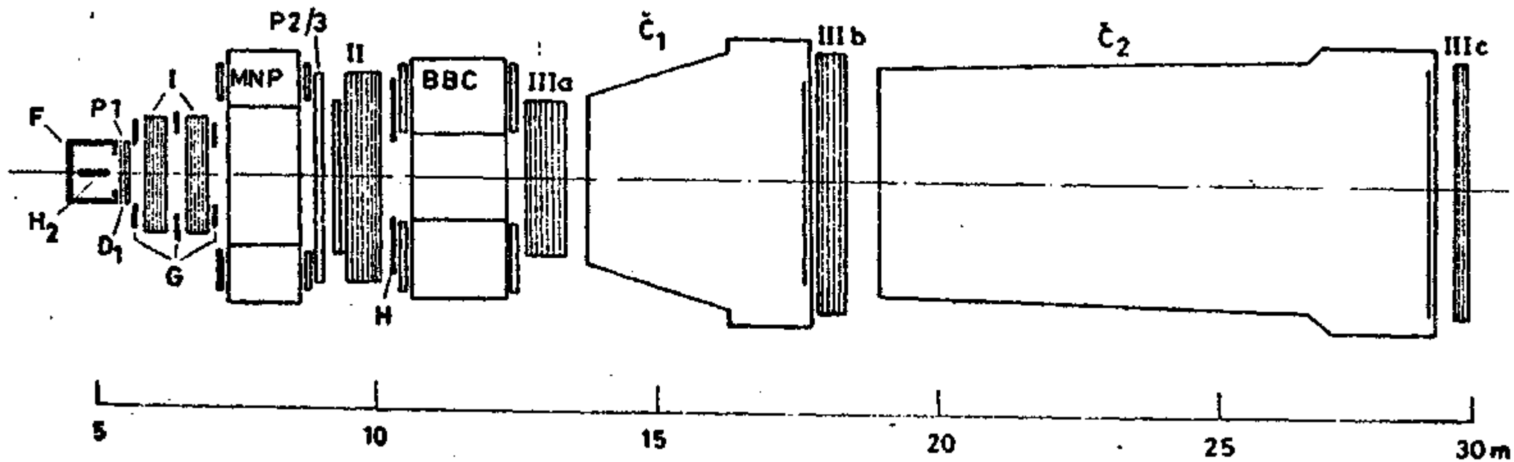

Fig. 1

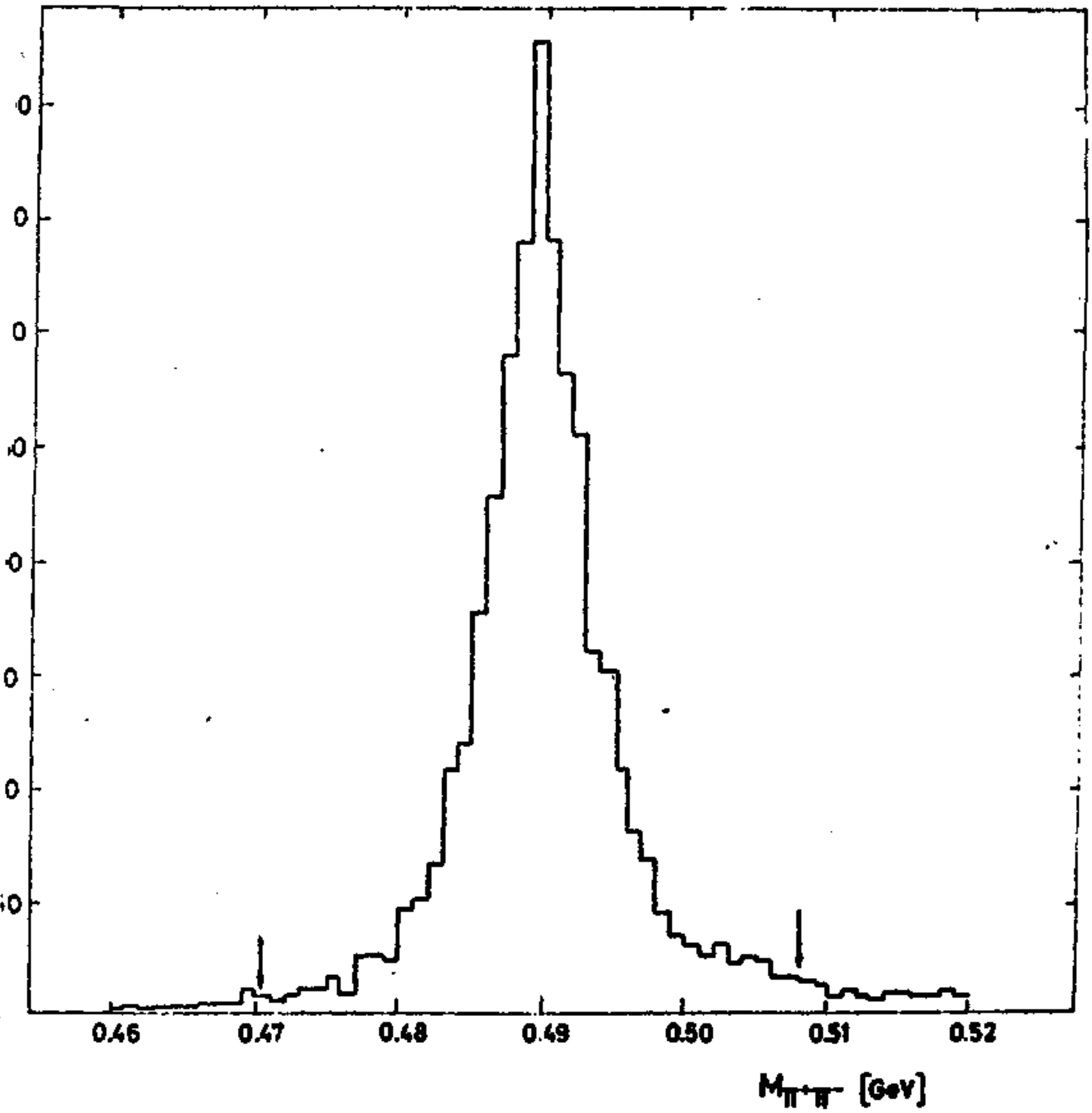

Fig. 2

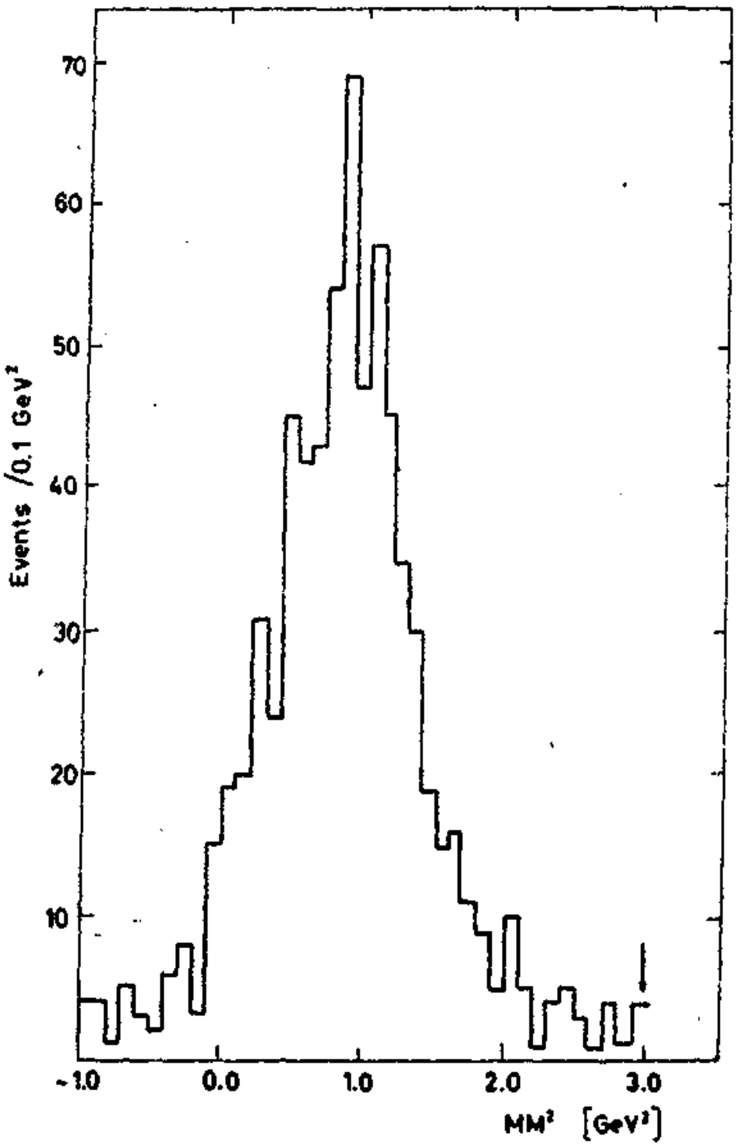

Fig. 3

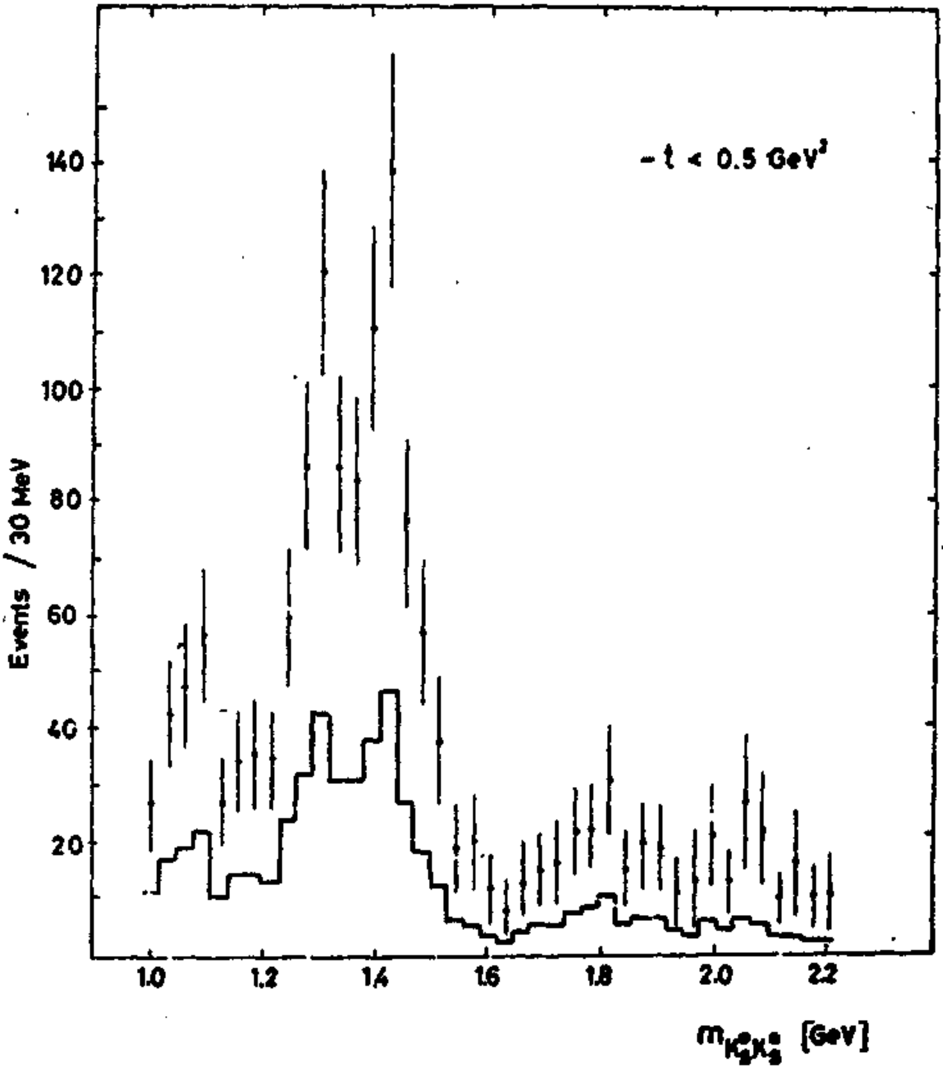

-t < 0.5 GeV²
Events / 30 MeV
20
40
60
80
100
120
140
1.0
1.2
1.4
1.6
1.8
2.0
2.2
$m_{K_S^0 K_S^0}$ [GeV]

Fig. 4

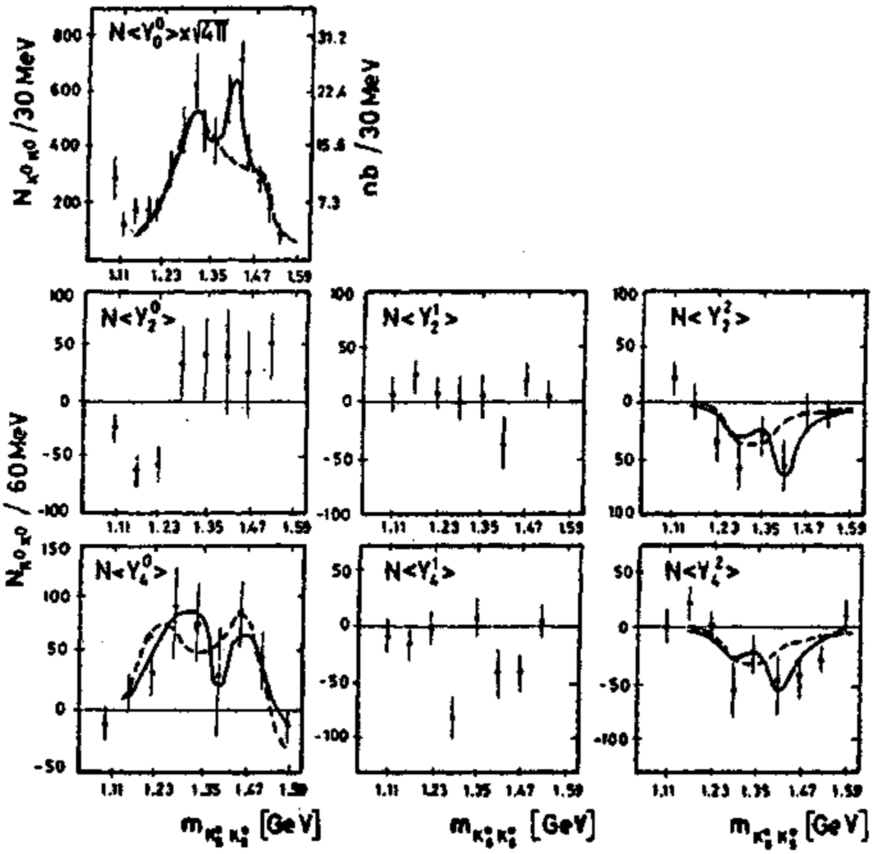

$N\langle Y_0^0\rangle \times\sqrt{4\pi}$
$N\langle Y_2^0\rangle$
$N\langle Y_2^1\rangle$
$N\langle Y_2^2\rangle$
$N\langle Y_4^0\rangle$
$N\langle Y_4^1\rangle$
$N\langle Y_4^2\rangle$
nb / 30 MeV
/ 30 MeV
/ 60 MeV
[GeV]

Fig. 5

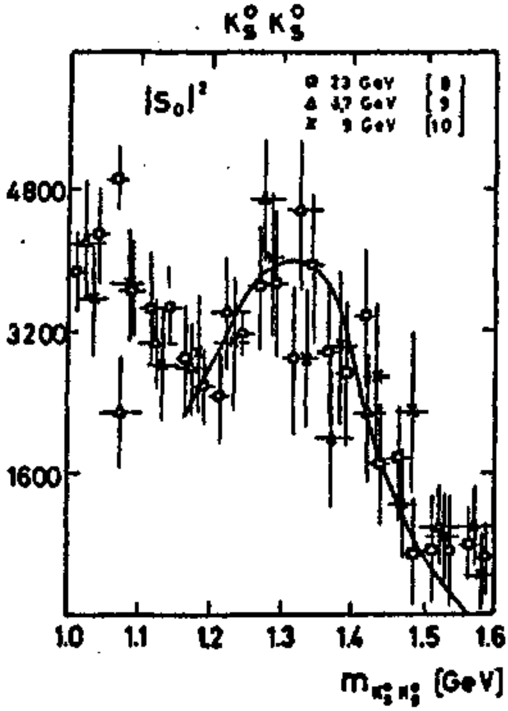
$K_S^0 K_S^0$
$|S_0|^2$
23 GeV [8]
5.7 GeV [9]
9 GeV [10]
4800
3200
1600
1.0
1.1
1.2
1.3
1.4
1.5
1.6
$m_{K_S^0 K_S^0}$ [GeV]

Fig. 6

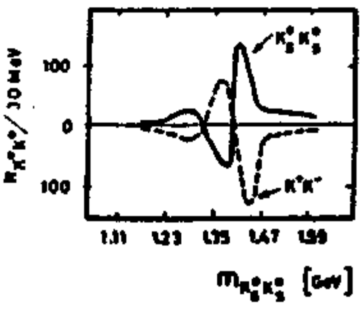
$K_S^0 K_S^0$
K^+K^-
100
0
100
1.11
1.23
1.35
1.47
1.59
$m_{K_S^0 K_S^0}$ [GeV]

Fig. 7

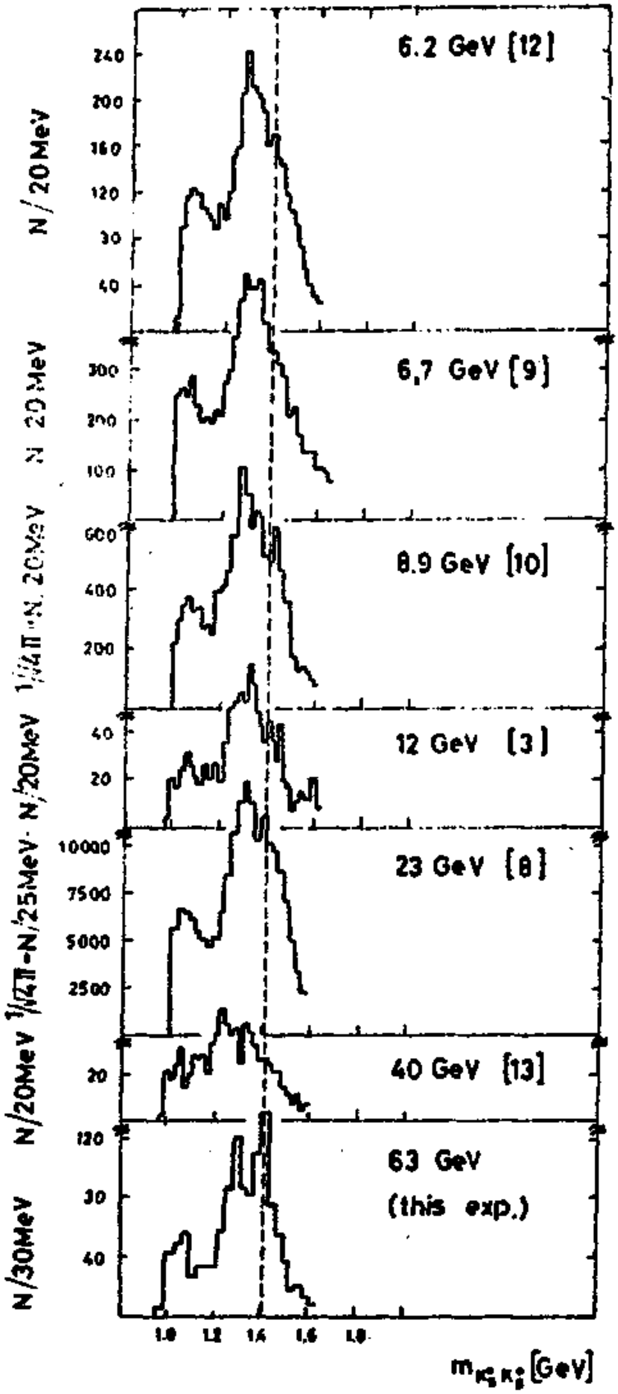

Fig. 8

IFJ Kraków, zam. 70/84 – 50 egz.